6th European Conference on Computational Mechanics (ECCM 6)
7th European Conference on Computational Fluid Dynamics (ECFD 7)
11–15 June 2018, Glasgow, UK

ON THE BENEFIT OF THE SUMMATION-BY-PARTS PROPERTY ON INTERIOR NODAL SETS

SIGRUN ORTLEB AND MABELLE FRANKE

Universität Kassel
Fachbereich Mathematik und Naturwissenschaften
Heinrich-Plett-Str. 40, 34132 Kassel, Germany
ortleb@mathematik.uni-kassel.de
http://www.mathematik.uni-kassel.de/~ortleb/

Key words: Discontinuous Galerkin, Summation-by-parts, Interior nodal distribution, Accuracy, Well-balancedness

Abstract. In this work, we review the potentially higher accuracy of the SBP schemes using Gauss nodes instead of Gauss-Lobatto nodes for the Navier-Stokes equations. To gain additional insight, we carry out a comparative Fourier type analysis for advection-diffusion equations discretized by the DG scheme on Gauss and Gauss-Lobatto nodes and two variants of viscous flux discretizations. Furthermore, the SBP property of DG schemes is used to construct a well-balanced and entropy conservative scheme on the classical Gauss nodes for the shallow water equations.

1 INTRODUCTION

Originating from the context of finite difference schemes, the summation-by-parts (SBP) property has been used to construct conservative and robust numerical methods for CFD simulations. By the special construction of SBP finite difference schemes, these methods mimic certain properties of the continuous equations in a similar manner as variational schemes such as Galerkin methods. Originally, the nodal sets in the construction of SBP schemes were chosen to contain a sufficient amount of boundary nodes. Recently, the SBP framework has been extended to nodal schemes on exclusively interior nodal sets such as discontinuous Galerkin (DG) schemes on Gauss points in one space dimension or on tensor-product grids, as well as triangular grid DG methods. SBP schemes are successfully applied to split-form equations which are used to establish certain secondary balances, e.g. regarding kinetic energy, either on nodal sets with a sufficient number of boundary nodes or on exclusively interior nodal sets. For specific problems, higher accuracy of the SBP schemes using Gauss nodes may be observed due to their higher degree of exactness for the corresponding quadrature rule. Here, we will review a result for a non-linear accoustic pressure wave. To gain additional insight, we carry out a comparative Fourier type analysis for advection-diffusion equations discretized by the DG scheme on Gauss and Gauss-Lobatto nodes and two variants of viscous flux discretizations. Although the quadrature rules on interior nodes have a higher degree of exactness,

split-form equations require additional boundary terms in order to obtain a consistent and conservative scheme, see e.g. [1]. The necessity to include boundary correction terms may be perceived as a drawback of exclusively interior nodes such as Gauss points. It is not a priori clear, which types of split forms still lead to conservation of both the primary conserved quantities as well as conservation of the targeted secondary ones. Here, we will show that the approach in [1] used to achieve kinetic energy preservation carries over to entropy preservation for the shallow water equations in skew-symmetric form, where the total energy is chosen as the entropy function.

2 THE DG SCHEME IN 1D IN SBP FRAMEWORK

Given a scalar hyperbolic conservation law in one space dimension

$$\frac{\partial}{\partial t}u(x,t) + \frac{\partial}{\partial x}f(u(x,t)) = 0, \quad t > 0,\ x \in \Omega = [a,b] \subset \mathbb{R}, \tag{1}$$

we generally obtain the DG scheme in weak form by multiplying the conservation law (1) with polynomial test functions on each grid cell and applying partial integration to the term containing the flux f. As the DG solution allows for discontinuities across cell boundaries, the flux evaluations on the boundaries are replaced by evaluations of a numerical flux function. In addition, integration is generally carried out by numerical quadrature rules.

As shown in [1], after a second partial integration, we obtain the strong form of the DG discretization in cell-wise fashion, transformed to a reference cell $I = [-1,1]$ with reference coordinate $\xi \in I$. This semi-discrete DG scheme reads

$$\frac{\Delta x}{2}\frac{d\underline{u}}{dt} + \underline{\underline{D}}\,\underline{f} = \underline{\underline{M}}^{-1}[(f_h - f^*)\underline{L}]_{-1}^{1}. \tag{2}$$

Here, Δx is the cell size, the solution vector $\underline{u} = (u_1, \ldots, u_{N+1})^T$ collects nodal values of the approximate solution at $N+1$ nodal points within a DG cell, i.e. $u_j \approx u\,(x(\xi_j), t)$, and the vector of flux values $\underline{f}$ is given by $\underline{f} = (f_1, \ldots, f_{N+1})^T$ with $f_j = f(u_j)$. Furthermore, f_h denotes an interpolation of the nonlinear function $f(u)$ at the DG nodes and f^* the numerical flux function. Using Lagrange polynomials $L_k(\xi)$ as the DG basis functions, the vector valued function $\underline{L}$ is given by $\underline{L}(\xi) = (L_1(\xi), \ldots, L_{N+1}(\xi))^T$ and the matrices $\underline{\underline{D}}$ and $\underline{\underline{M}}$ are defined by their entries $D_{jk} = L_k'(\xi_j)$ and $M_{jk} = \int_{-1}^{1} L_j L_k d\xi = M_{kj}$.

According to [2], Definition 2, a scheme of the form (2) is an SBP scheme, or else, the matrix $\underline{\underline{D}}$ is an SBP operator, if the subsequent conditions are fulfilled.

1. The matrix $\underline{\underline{D}}$ is an approximation to $\frac{\partial}{\partial \xi}$ with $\underline{\underline{D}}\,\underline{\xi}^j = j\underline{\xi}^{j-1}$ for all $0 \leq j \leq q$, where q denotes the degree of the approximation to the first derivative and $\underline{\xi}^j = (\xi_1^j, \ldots, \xi_{N+1}^j)^T$.

2. The matrix $\underline{\underline{M}}$ is symmetric and positive definite.

3. Integration by parts is mimicked by $\underline{\underline{M}}\,\underline{\underline{D}} + \underline{\underline{D}}^T\underline{\underline{M}} = \underline{\underline{B}} = \underline{\underline{B}}^T$, where $\underline{\underline{B}}$ is an interface and boundary operator with the property $(\underline{\xi}^l)^T\underline{\underline{B}}\,\underline{\xi}^m = [\xi^{l+m}]_{-1}^{1}$ for all $0 \leq l, m \leq r$,

where $r \geq q$ denotes the degree of the SAT terms used for imposition of boundary and interface conditions.

For the DG scheme (2) written for a spatial variable ξ on the reference cell $[-1, 1]$ we now have the following SBP property, see [1]. The matrix $\underline{\underline{D}}$ approximates $\frac{\partial}{\partial \xi}$ to degree $q = N$ and the degree of $\underline{\underline{B}}$ is $r = q = N$ as well. Furthermore, given a function $g(\xi)$ with point-wise values $\underline{g}$, the interface and boundary operator $\underline{\underline{B}}$ acts on $\underline{g}$ as

$$\underline{\underline{B}}\,\underline{g} = [g_h \underline{L}]_{-1}^{1},$$

where $g_h = \sum_{j=1}^{N+1} g_j L_j(\xi)$ denotes polynomial interpolation of the point-wise values $\underline{g}$. Furthermore, the entries of $\underline{\underline{B}}$ are given by $B_{jk} = [L_j L_k]_{-1}^{1}$.

In case of Gauss-Lobatto (GL) nodes, the matrix $\underline{\underline{B}}$ is simply given by

$$\underline{\underline{B}}_{GL} = \mathrm{diag}\{-1, 0, \ldots, 0, 1\}\,.$$

For the classical Gauss nodes (G) the DG schemes of order $N = 1$ and $N = 2$ yield

$$\underline{\underline{B}}_{G,N=1} = \mathrm{diag}\{-\sqrt{3}, \sqrt{3}\}, \quad \underline{\underline{B}}_{G,N=2} = \begin{pmatrix} -\frac{1}{\xi^3} & \frac{1-\xi^2}{\xi^3} & 0 \\ \frac{1-\xi^2}{\xi^3} & 0 & \frac{\xi^2-1}{\xi^3} \\ 0 & \frac{\xi^2-1}{\xi^3} & \frac{1}{\xi^3} \end{pmatrix},\ \xi = \sqrt{\frac{3}{5}}\,.$$

If the chosen quadrature rule exactly integrates polynomials of degree $2N$, e.g. for Gauss nodes, we have $M_{jk} = \delta_{jk}\omega_j$ due to exact integration of the integrals. Hence, $\underline{\underline{M}}$ is diagonal in this case and $\underline{\underline{D}}$ is called a diagonal-norm SBP operator. Non-diagonal matrices $\underline{\underline{M}}$ lead to so-called non-diagonal norm SBP operators. However, if Gauss-Lobatto quadrature is used to compute the mass matrix, we obtain a diagonal mass matrix with $M_{jk} = \delta_{jk}\omega_j$ and hence a diagonal norm SBP operator. This is also referred to as mass lumping.

Choosing the classical Gauss nodes which do not contain the interval end points $\xi = -1$ and $\xi = 1$ yields exact integration of polynomials up to degree $2N + 1$. Due to the improved accuracy of the resulting DG scheme, these points might be preferred to the Gauss-Lobatto variant with mass lumping. Higher efficiency of Gauss nodes especially for a non-linear example based on the two-dimensional Euler equations is numerically demonstrated in [3]. However, as also stated in [3], in addition to the lower cost based on the fact that boundary interpolation is not required, the DG scheme on Gauss-Lobatto nodes also allows larger time steps in case of explicit time integration. Time steps may be taken roughly twice as large in comparison to Gauss nodes as shown in [4]. Further subtleties arise as Gauss integration may increase robustness for non-linear problems and underresolved simulations, see e.g. [4, 5]. Hence, the question of efficiency will depend on the specific application including accuracy requirements.

3 AN EXAMPLE OF INCREASED ACCURACY FOR GAUSS NODES

The following test case studied in [6, 1] is based on the compressible Navier-Stokes equations. The equations to be solved are given by

$$\frac{\partial}{\partial t}U + \frac{\partial}{\partial x}F(U) = \frac{\partial}{\partial x}F^{visc}(U, U_x),$$

where the conservative quantities are collected in $U = (\rho, \rho v, \rho e)^T$, containing the density ρ, the velocity v and the specific total energy e. The inviscid fluxes are given by $F(U) = (\rho v, \rho v^2 + p, v(\rho e + p))^T$, with $p = (\gamma - 1)\rho(e - v^2/2)$ the pressure and $F^{visc}(U, U_x) = \left(0, \mu\frac{4}{3}v_x, \mu\frac{4}{3}vv_x + kT_x\right)^T$ contains the viscous fluxes. Herein, the viscosity coefficient $\mu = \mu(T)$ possibly depends on the temperature $T = \frac{\gamma}{c_p}e$, where c_p is the specific heat at constant pressure. The head conduction coefficient is furthermore given by $k = \frac{c_p\mu}{Pr}$, with the Prandtl number Pr. The initial conditions for the acoustic pressure wave are given by the initial density, velocity and pressure distribution

$$\rho(x, 0) = 1, \quad v(x, 0) = 1, \quad p(x, 0) = 1 + 0.1\sin(2\pi x)$$

on the computational domain $\Omega = [0, 1]$ with periodic boundary conditions. The viscosity coefficient is set to $\mu = 0.002$ and the Prandtl number is $Pr = 0.72$. The viscous terms are discretized by the BR2 approach developed by Bassi and Rebay, see [7]. The numerical computations are carried out until $t_{end} = 20$ to study long time integration. Fig. 1 shows the output of the kinetic energy preserving, skew-symmetric DG schemes for $N = 1$ in case of Gauss as well as Gauss-Lobatto nodes as specified in [1].

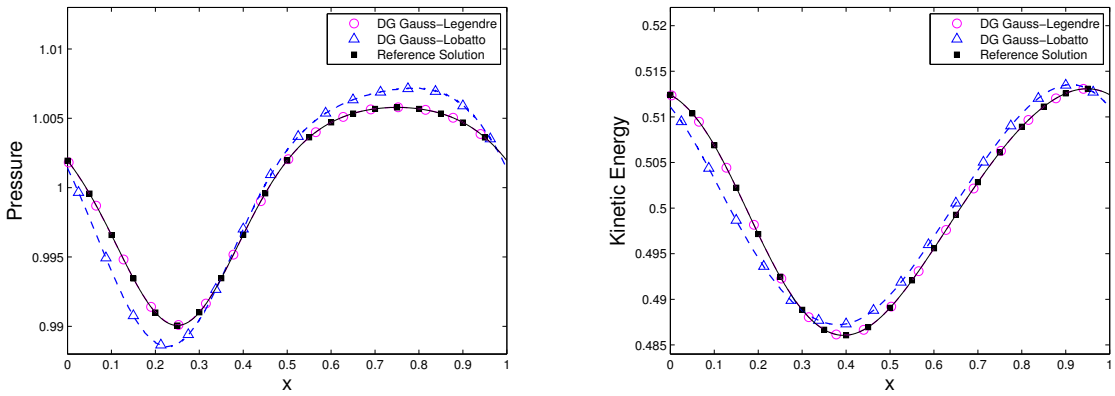

Figure 1: DG scheme using skew-symmetric terms for $N = 1$, Gauss (40 cells) vs. Gauss-Lobatto nodes (80 cells) using kinetic energy preserving flux f_C^*. Left: pressure. Right: kinetic energy.

In a comparison with a reference solution obtained by the standard DG scheme for a polynomial degree $N = 3$ and 500 cells, the Gauss-Lobatto variant clearly is not as accurate as the Gauss variant on the coarser grid as shown in Fig. 1 where the DG solution with Gauss nodes almost cannot be distinguished from the reference solution.

4 FOURIER ANALYSIS

We will now study the increased accuracy for Gauss nodes via a Fourier analysis carried out on a simplified linear model. This simplified model equation is naturally given by a linear advection-diffusion equation with a small diffusion coefficient $\epsilon > 0$. For a linear advection-diffusion equation of the form

$$\begin{aligned} u_t + u_x &= \epsilon u_{xx}, \quad x \in [0, 2\pi],\ t > 0, \\ u(x,0) &= e^{i\omega x}, \quad x \in [0, 2\pi], \end{aligned}$$

supplemented by periodic boundary conditions, the exact solution is given by

$$u(x,t) = e^{-(i\omega + \epsilon\omega^2)t} e^{i\omega x}\,. \tag{3}$$

A standard DG discretization based on the corresponding system of first order PDEs,

$$\begin{aligned} u_t + u_x &= \epsilon q_x, , \\ q &= u_x, \end{aligned} \tag{4}$$

is then given by

$$\begin{aligned} \frac{\Delta x}{2}\underline{u}_t + \underline{\underline{D}}\,\underline{u} - \epsilon \underline{\underline{D}}\,\underline{q} &= \underline{\underline{M}}^{-1}\left([(u_h - u^*_{adv})\underline{L}]^1_{-1} - \epsilon[(q_h - q^*)\underline{L}]^1_{-1}\right)\,, \\ \frac{\Delta x}{2}\underline{q} - \underline{\underline{D}}\,\underline{u} &= -\underline{\underline{M}}^{-1}[(u_h - u^*)\underline{L}]^1_{-1}\,. \end{aligned}$$

As numerical flux functions, an upwind flux $u^*_{adv} = u^-$ is chosen for the advective term, while the viscous term is discretized by either the BR2 fluxes $q^* = \frac{1}{2}(q^- + q^+)$ and $u^* = \frac{1}{2}(u^- + u^+)$ or the LDG approach $q^* = q^+$ and $u^* = u^-$.

A Fourier analysis, as carried out in [8, 9], assumes a uniform grid with periodic boundary conditions. On the grid cell C_m, the numerical solution is assumed to be of the form

$$\underline{u}_m(t) = \underline{\hat{u}}(t) e^{i\omega x_m}\,. \tag{5}$$

On the other hand, the DG scheme (4) can be written as

$$\begin{aligned} \frac{d\underline{u}_m}{dt} = &\frac{1}{\Delta x}\left(\underline{\underline{A}}_1\,\underline{u}_m + \underline{\underline{A}}_2\,\underline{u}_{m-1}\right) \\ &- \frac{\epsilon}{\Delta x^2}\left(\underline{\underline{A}}_3\,\underline{u}_{m-2} + \underline{\underline{A}}_4\,\underline{u}_{m-1} + \underline{\underline{A}}_5\,\underline{u}_m + \underline{\underline{A}}_6\,\underline{u}_{m+1} + \underline{\underline{A}}_7\,\underline{u}_{m+2}\right)\,. \end{aligned} \tag{6}$$

Substituting (5) into (6) yields the ODE

$$\frac{d\underline{\hat{u}}}{dt} = \underline{\underline{G}}\,\underline{\hat{u}}\,,$$

with the amplification matrix

$$\underline{\underline{G}} = \frac{1}{\Delta x}\left(\underline{\underline{A}}_1 + \underline{\underline{A}}_2 e^{-i\omega\Delta x}\right) - \frac{\epsilon}{\Delta x^2}\left(\underline{\underline{A}}_3 e^{-2i\omega\Delta x} + \underline{\underline{A}}_4 e^{-i\omega\Delta x} + \underline{\underline{A}}_5 + \underline{\underline{A}}_6 e^{i\omega\Delta x} + \underline{\underline{A}}_7 e^{2i\omega\Delta x}\right).$$

An explicit representation of the DG solution may now be obtained by computing the eigenvalues and eigenvectors of $\underline{\underline{G}}$. Differences may be expected for choosing Gauss or Gauss-Lobatto nodes as well as depending on the numerical flux functions. For $N = 1$, using symbolic computations with Mathematica, we obtain the following eigenvalues.
Gauss nodes, LDG:

$$\lambda_1 = -(i+\epsilon\omega)\omega - \frac{\omega^4}{72}\Delta x^3 + \frac{\omega^5}{540}(3i+\epsilon\omega)\Delta x^4 + \mathcal{O}(\Delta x^5)$$
$$\lambda_2 = -\frac{36\epsilon}{\Delta x^2} - \frac{6}{\Delta x} + 3(i+\epsilon\omega)\omega + \mathcal{O}(\Delta x)$$

Gauss-Lobatto nodes, LDG:

$$\lambda_1 = -(i+\epsilon\omega)\omega + \frac{\omega^3}{6}(i+2\epsilon\omega)\Delta x^2 - \frac{\omega^4}{8}\Delta x^3 + \mathcal{O}(\Delta x^4)$$
$$\lambda_2 = -\frac{4\epsilon}{\Delta x^2} - \frac{2}{\Delta x} + (i-\epsilon\omega)\omega + \mathcal{O}(\Delta x^2)$$

Gauss nodes, BR2:

$$\lambda_1 = -(i+\epsilon\omega)\omega - \frac{\omega^4}{12}\epsilon\Delta x^2 + \frac{\omega^4}{72}(i-2\epsilon\omega)^2\Delta x^3 + \mathcal{O}(\Delta x^4)$$
$$\lambda_2 = -\frac{6}{\Delta x} + 3(i-3\epsilon\omega)\omega + \mathcal{O}(\Delta x)$$

Gauss-Lobatto nodes, BR2:

$$\lambda_1 = -(i+\epsilon\omega)\omega + \frac{\omega^3}{12}(2i+\epsilon\omega)\Delta x^2 + \frac{\omega^4}{8}\Delta x^3 + \mathcal{O}(\Delta x^4)$$
$$\lambda_2 = -\frac{2}{\Delta x} + (i-\epsilon\omega)\omega + \mathcal{O}(\Delta x^2)$$

We may observe that for Δx sufficiently small, the eigenvalue λ_2 has negative real part and $|Re(\lambda_2)|$ increases with decreasing cell size Δx. The corresponding term in the ODE solution is thus damped out in time. In addition, for the Gauss variants, $|Re(\lambda_2)|$ is larger in comparison to the corresponding Gauss-Lobatto variant, suggesting increased stiffness of the ODE for Gauss nodes. Regarding the exact solution (3), we need $\lambda_1 = -(i+\epsilon\omega)\omega + \mathcal{O}(\Delta x)$ for consistency, which is fulfilled by all of the above schemes. For the LDG scheme, a difference in accuracy is manifested by the fact that λ_1 is an $\mathcal{O}(\Delta x^3)$ approximation to $-(i+\epsilon\omega)\omega$ for Gauss nodes while the approximation is only of order $\mathcal{O}(\Delta x^2)$ for Gauss-Lobatto nodes. For the BR2 scheme, λ_1 is an $\mathcal{O}(\Delta x^2)$ approximation of $-(i+\epsilon\omega)\omega$ in both cases. However, for the Gauss variant, the second order term nearly vanishes for the advection-dominated situation $\epsilon \ll 1$, thus again resulting in potentially higher accuracy of the DG scheme on Gauss nodes.

5 ENTROPY PRESERVING WELL-BALANCED DG SCHEMES ON GAUSS NODES FOR SHALLOW WATER FLOW

Though sufficient accuracy ot the numerical solution is of crucial importance and may be achieved at a lower computational cost for Gauss nodes, removing the cell boundary nodes from the nodal set may prevent other advantageous properties of the discretization. While classical SBP schemes including boundary nodes are successfully applied to split-form PDEs to guarantee the preservation of secondary quantities, the general viability of generalized SBP schemes on interior node distributions still needs to be clarified in this regard. In [10], the DG scheme on Gauss-Lobatto nodes is used to construct an entropy preserving numerical method for the shallow water equations with is provably well-balanced, i.e. preserves lake at rest stationary solutions. Furthermore, based on the so-called correction procedure via reconstruction (CPR), generalized SBP schemes with this property have recently been constructed in [11]. In the following, we derive an entropy preserving, well-balanced DG scheme on Gauss nodes for the shallow water equations along the investigations in [10].

5.1 Skew-symmetric formulation of the shallow water equations

The classical conservative form of the shallow water equations with non-constant bottom topography is given by

$$h_t + (hv)_x = 0, \tag{7}$$

$$(hv)_t + \left(hv^2 + \frac{1}{2} g h^2 \right)_x = -ghb_x, \tag{8}$$

where h denotes the water height above the bottom elevation b, while g denotes the gravitational constant and v the flow velocity. Using product rules, it is possible to derive from the above equations the skew-symmetric formulation of the momentum equation

$$\frac{1}{2}\left[(hv)_t + hv_t\right] + \frac{1}{2}\left[(hv^2)_x + hvv_x\right] + gh(h+b)_x = 0. \tag{9}$$

In [10], this formulation is used to derive an entropy preserving, well-balanced DG scheme on Gauss-Lobatto nodes using the summation-by parts property. In this work, we show that the same derivations can be carried out for the classical Gauss nodes. Hereby, entropy preservation refers to the preservation of total energy $e = k + p$, composed of the kinetic energy $k = \frac{1}{2} h v^2$ and the potential energy $p = \frac{1}{2} g h^2 + ghb$. The total energy represents an entropy function for the shallow water equations. Setting $\underline{u}_1 = \underline{h}$ und $\underline{u}_2 = \underline{\underline{h}}\,\underline{v}$ we obtain the DG scheme

$$\frac{\Delta x}{2} \frac{d\underline{u}_1}{dt} + \underline{\underline{D}}\,\underline{f}_1 = \underline{\underline{M}}^{-1}[(f_{1,h} - f_1^*)\underline{L}]_{-1}^{1}\,, \tag{10}$$

$$\frac{\Delta x}{2}\frac{1}{2}\left(\frac{d\underline{u}_2}{dt} + \underline{\underline{h}}\frac{d\underline{v}}{dt}\right) + \frac{1}{2}\left(\underline{\underline{D}}\,\underline{\underline{h}}\,\underline{v}^2 + \underline{\underline{hv}}\,\underline{\underline{D}}\underline{v}\right) + g\underline{\underline{h}}\,\underline{\underline{D}}(\underline{h} + \underline{b}) = \underline{\underline{M}}^{-1}[(k_h - k^*)\underline{L}]_{-1}^{1}, \tag{11}$$

where k_h and k^* are not yet specified.

Multiplying the above semi-discrete continuity equation by $\frac{1}{2}\underline{\underline{v}}$ and adding this to the skew-symmetric momentum equation yields, due to time continuity,

$$\begin{aligned}&\frac{\Delta x}{2}\frac{d\underline{u}_2}{dt} + \underline{\underline{D}}\,\underline{f}_{-2} + \frac{1}{2}\underline{s}_{hv,v} + \frac{g}{2}\underline{s}_{h,h} + g\underline{\underline{h}}\,\underline{\underline{D}}\,\underline{b} \\ &= \underline{\underline{M}}^{-1}\left([(k_h - k^*)\underline{L}]_{-1}^1 + \frac{1}{2}\underline{\underline{v}}[(f_{1,h} - f_1^*)\underline{L}]_{-1}^1\right),\end{aligned} \tag{12}$$

where $\underline{s}_{hv,v} = -\underline{\underline{D}}\,\underline{\underline{h}}\,\underline{\underline{v}}^2 + \underline{\underline{hv}}\,\underline{\underline{Dv}} + \underline{\underline{v}}\,\underline{\underline{D}}\,\underline{\underline{hv}}$ and $\underline{s}_{h,h} = -\underline{\underline{D}}\,\underline{\underline{h}}^2 + 2\underline{\underline{h}}\,\underline{\underline{Dh}}$.

5.2 Mass and momentum balance

Now, the semi-discrete continuity equation is given precisely by the standard DG scheme, hence mass preservation is guaranteed.

For the momentum balance we consider the discrete terms $\underline{s}_{\alpha,\beta} = -\underline{\underline{D}}\,\underline{\underline{\alpha}}\,\underline{\beta} + \underline{\underline{\alpha}}\,\underline{\underline{D}}\,\underline{\beta} + \underline{\underline{\beta}}\,\underline{\underline{D}}\,\underline{\alpha}$ mimicking the product rule. We have

$$\begin{aligned}\underline{1}^T\underline{\underline{M}}\,\underline{s}_{\alpha,\beta} &= \underline{1}^T\underline{\underline{M}}\,\left(-\underline{\underline{D}}\,\underline{\underline{\alpha}}\,\underline{\beta} + \underline{\underline{\alpha}}\,\underline{\underline{D}}\,\underline{\beta} + \underline{\underline{\beta}}\,\underline{\underline{D}}\,\underline{\alpha}\right) \\ &= \underline{1}^T\left[\left(\underline{\underline{D}}^T\underline{\underline{M}} - \underline{\underline{B}}\right)\underline{\underline{\alpha}}\,\underline{\beta} + \underline{\underline{\alpha}}\left(\underline{\underline{B}} - \underline{\underline{D}}^T\underline{\underline{M}}\right)\underline{\beta} + \underline{\underline{\beta}}\,\underline{\underline{M}}\,\underline{\underline{D}}\,\underline{\alpha}\right] \\ &= -\underline{1}^T\underline{\underline{B}}\,\underline{\underline{\alpha}}\,\underline{\beta} + \underline{\alpha}^T\,\underline{\underline{B}}\,\underline{\beta}\,.\end{aligned} \tag{13}$$

In case of interior node distributions, the boundary matrices $\underline{\underline{B}}$ are generally not diagonal and $\underline{1}^T\underline{\underline{M}}\,\underline{s}_{\alpha,\beta} \neq \underline{0}$. Therefore, boundary correction terms have to be added to the right-hand side of the DG scheme. We have $\underline{1}^T\underline{\underline{M}}\,\underline{s}_{hv,v} = \underline{1}^T\underline{\underline{M}}\,\underline{s}_{v,hv} = -\underline{1}^T\underline{\underline{B}}\,\underline{\underline{hv}}^2 + \underline{v}^T\,\underline{\underline{B}}\,\underline{f}_1$ and $\underline{1}^T\underline{\underline{M}}\,\underline{s}_{h,h} = -\underline{1}^T\underline{\underline{B}}\,\underline{h}^2 + \underline{h}^T\,\underline{\underline{B}}\,\underline{h}$.

From (12) we derive that for constant bottom topography, $\underline{\underline{D}}\,\underline{b} = \underline{0}$, the contribution of the volume terms to the change of momentum within a DG cell sums up to

$$\underline{1}^T\underline{\underline{M}}\left(\underline{\underline{D}}\,\underline{f}_2 + \frac{1}{2}\underline{s}_{hv,v} + \frac{g}{2}\underline{s}_{h,h}\right) = \frac{1}{2}\underline{1}^T\underline{\underline{B}}\,\underline{\underline{h}}\,\underline{\underline{v}}^2 + \frac{1}{2}\underline{v}^T\underline{\underline{B}}\,\underline{f}_1 + \frac{g}{2}\underline{h}^T\underline{\underline{B}}\,\underline{h}\,. \tag{14}$$

Furthermore, as $\underline{1}^T\left(\frac{1}{2}\underline{\underline{v}}[(f_{1,h} - f_1^*)\underline{L}]_{-1}^1\right) = \frac{1}{2}\underline{v}^T\underline{\underline{B}}\,\underline{f}_1 - \frac{1}{2}[v_h f_1^*]_{-1}^1$, we may choose

$$\begin{aligned}k_h &= \frac{1}{2}\left((hv^2)_h + g(h_h)^2\right) = f_{2,h} - \frac{1}{2}(hv^2)_h + \frac{g}{2}\left((h_h)^2 - (h^2)_h\right)\,, \\ k^*(\pm 1) &= f_2^* - \frac{1}{2}v_h(\pm 1)f_1^*\,,\end{aligned}$$

in order to obtain for the surface terms

$$\begin{aligned}&\underline{1}^T\left([(k_h - k^*)\underline{L}]_{-1}^1 + \frac{1}{2}\underline{\underline{v}}[(f_{1,h} - f_1^*)\underline{L}]_{-1}^1\right) \\ &= \frac{1}{2}\underline{1}^T\underline{\underline{B}}\,\underline{\underline{hv}}^2 + \frac{g}{2}\underline{h}^T[h_h\underline{L}]_{-1}^1 - \left[f_2^* - \frac{1}{2}v_h f_1^*\right]_{-1}^1 + \frac{1}{2}\underline{v}^T\underline{\underline{B}}\,\underline{f}_1 - \frac{1}{2}[v_h f_1^*]_{-1}^1 \\ &= \frac{1}{2}\underline{1}^T\underline{\underline{B}}\,\underline{\underline{hv}}^2 + \frac{g}{2}\underline{h}^T\underline{\underline{B}}\,\underline{h} + \frac{1}{2}\underline{v}^T\underline{\underline{B}}\,\underline{f}_1 + [f_2^*]_{-1}^1\,.\end{aligned} \tag{15}$$

Comparing (14) and (15), the change of momentum within a cell directly corresponds to momentum fluxes across the cell boundaries. In addition, the numerical flux f_2^* is unique on each cell boundary. Therefore, for constant bottom topography, momentum is conserved.

The final form of the skew-symmetric semi-discrete momentum equation is given by

$$\frac{\Delta x}{2}\frac{d\underline{u}_2}{dt} + \underline{\underline{D}}\,\underline{f}_2 + \frac{1}{2}\underline{s}_{hv,v} + \frac{g}{2}\underline{s}_{h,h} + g\underline{h}\,\underline{\underline{D}}\,\underline{b} = \underline{\underline{M}}^{-1}[(f_{2,h} - f_2^*)\underline{L}]_{-1}^{1} + \underline{\underline{M}}^{-1}\underline{s}^{bc}\,, \tag{16}$$

with the cell boundary correction term

$$\underline{s}^{bc} = \frac{1}{2}\underline{v}[(f_{1,h} - f_1^*)\underline{L}]_{-1}^{1} - \frac{1}{2}\left[\left((hv^2)_h - v_h f_1^* - g(h_h)^2 + g(h^2)_h\right)\underline{L}\right]_{-1}^{1}\,.$$

5.3 Entropy conservation

An entropy function for the shallow water equations is given by the total energy composed of the kinetic energy $k = \frac{1}{2}hv^2$ and the potential energy $p = \frac{1}{2}gh^2 + ghb$. The semi-discrete kinetic energy balance can be reconstructed from the initial momentum discretization (11) multiplied by $\underline{v}$, since $\frac{d}{dt}\underline{k} = \frac{1}{2}(\underline{v}\frac{d\underline{u}_2}{dt} + \underline{u}_2\frac{d\underline{v}}{dt})$. We have

$$\frac{\Delta x}{2}\frac{d\underline{k}}{dt} + \frac{1}{2}\underline{v}\left(\underline{\underline{D}}\,\underline{h}\,\underline{v}^2 + \underline{hv}\,\underline{\underline{D}}\,\underline{v}\right) + g\underline{h}\,\underline{v}\,\underline{\underline{D}}(\underline{h} + \underline{b}) = \underline{\underline{M}}^{-1}\underline{v}[(k_h - k^*)\underline{L}]_{-1}^{1}\,.$$

The semi-discrete potential energy balance can be obtained from the semi-discrete continuity equation multiplied by $g(\underline{h} + \underline{b})$ since $\frac{d}{dt}\underline{p} = g(\underline{h} + \underline{b})\frac{d\underline{h}}{dt}$. We obtain

$$\frac{\Delta x}{2}\frac{d\underline{p}}{dt} + g(\underline{h} + \underline{b})\underline{\underline{D}}\,\underline{f}_1 = \underline{\underline{M}}^{-1}g(\underline{h} + \underline{b})[(f_{1,h} - f_1^*)\underline{L}]_{-1}^{1}\,.$$

For the total energy, we have thus

$$\begin{aligned}&\frac{\Delta x}{2}\frac{d\underline{e}}{dt} + \underline{\underline{D}}\left(\frac{1}{2}\underline{hv}^3 + g\underline{u}_2(\underline{h} + \underline{b})\right) + \frac{1}{2}\underline{s}_{v,hv^2} + g\underline{s}_{hv,h+b}\\ &= \underline{\underline{M}}^{-1}\underline{v}[(k_h - k^*)\underline{L}]_{-1}^{1} + \underline{\underline{M}}^{-1}g(\underline{h} + \underline{b})[(f_{1,h} - f_1^*)\underline{L}]_{-1}^{1}\,.\end{aligned}$$

Considering the cell means, using (13), we have

$$\begin{aligned}\underline{1}^T\underline{\underline{M}}\frac{\Delta x}{2}\frac{d\underline{e}}{dt} &= -\frac{1}{2}\underline{v}^T\underline{\underline{B}}\underline{hv}^2 - g\underline{u}_2^T\underline{\underline{B}}(\underline{h} + \underline{b}) + \underline{v}^T[(k_h - k^*)\underline{L}]_{-1}^{1} + g(\underline{h} + \underline{b})^T[(f_{1,h} - f_1^*)\underline{L}]_{-1}^{1}\\ &= \underline{v}^T\left[\left(\frac{g}{2}(h_h)^2 - k^*\right)\underline{L}\right]_{-1}^{1} - g(\underline{h} + \underline{b})^T[f_1^*\underline{L}]_{-1}^{1}\,.\end{aligned}$$

Now, at an interface the sum of ingoing and outgoing fluxes has to be zero. At such an interface between to cells C_m, C_{m+1}, we define the jump and the arithmetic mean of a quantity a_h as $[[a_h]] = a_h^{m+1}(-1) - a_h^m(1)$ and $\{\{a_h\}\} = \frac{1}{2}\left(a_h^{m+1}(-1) + a_h^m(1)\right)$. Thus, at

an interface, we obtain

$$
\begin{aligned}
&(\underline{v}^{m+1})^T \left(\left(\frac{g}{2}(h_h^{m+1})^2(-1) - k^{*,m+1}(-1) \right) \underline{L}(-1) \right) - g(\underline{h}^{m+1} + \underline{b}^{m+1})^T f_1^* \underline{L}(-1) \\
&- (\underline{v}^{m})^T \left(\left(\frac{g}{2}(h_h^{m})^2(1) - k^{*,m}(1) \right) \underline{L}(1) \right) + g(\underline{h}^{m} + \underline{b}^{m})^T f_1^* \underline{L}(1) \\
&= \frac{g}{2}[[(v_h)(h_h)^2]] - f_2^*[[v_h]] + \frac{1}{2} f_1^*[[(v_h)^2]] - g f_1^*[[(h+b)_h]] \,.
\end{aligned}
$$

As $[[a_h b_h]] = \{\{a_h\}\}[[b_h]] + [[a_h]]\{\{b_h\}\}$, and assuming a continuous bottom topography, i.e. $[[b_h]] = 0$, we may rewrite this as

$$
\begin{aligned}
&g\{\{v_h\}\}\{\{h_h\}\}[[h_h]] + \frac{g}{2}\{\{(h_h)^2\}\}[[v_h]] - f_2^*[[v_h]] + f_1^*\{\{v_h\}\}[[v_h]] - g f_1^*[[h_h]] \\
&= g\left(\{\{v_h\}\}\{\{h_h\}\} - f_1^*\right)[[h_h]] + \left(\frac{g}{2}\{\{(h_h)^2\}\} - f_2^* + f_1^*\{\{v_h\}\} \right)[[v_h]] \stackrel{!}{=} 0
\end{aligned}
$$

Since $[[h_h]]$ and $[[v_h]]$ may cancel out independently, we obtain the energy conservative numerical flux

$$
f^* = \begin{pmatrix} f_1^* \\ f_2^* \end{pmatrix} = \begin{pmatrix} \{\{h_h\}\}\{\{v_h\}\} \\ \{\{h_h\}\}\{\{v_h\}\}^2 + \frac{g}{2}\{\{(h_h)^2\}\} \end{pmatrix} .
$$

Using this numerical flux, an entropy conserving DG scheme on Gauss nodes is constructed.

5.4 Well-balancedness

Well-balancedness for lake at rest situations $v \equiv 0$ and $h + b \equiv const$ and a continuous bottom topography can be proven for the entropy conserving DG scheme on Gauss nodes as follows. Due to $v \equiv 0$, the continuity equation (10) directly reduces to stationary water height, i.e. $\frac{\Delta x}{2}\frac{d\underline{u}_1}{dt} = 0$. The momentum equation (12) yields

$$
\begin{aligned}
\frac{\Delta x}{2}\frac{d\underline{u}_2}{dt} &= -g\underline{\underline{h}}\,\underline{\underline{D}}\,(\underline{h} + \underline{b}) + \underline{\underline{M}}^{-1}\left[\left(\frac{g}{2}(h_h)^2 - f_2^* \right) \underline{L} \right]_{-1}^{1} \\
&= \underline{\underline{M}}^{-1}\left[\left(\frac{g}{2}(h_h)^2 - \frac{g}{2}\{\{(h_h)^2\}\} \right) \underline{L} \right]_{-1}^{1} .
\end{aligned}
$$

Now, since we assume a continuous bottom topography, hence $[[b]] = 0$, the lake at rest condition $[[h + b]] = 0$ yields $[[h]] = 0$ and thus

$$
\left[\left(\frac{g}{2}(h_h)^2 - \frac{g}{2}\{\{(h_h)^2\}\} \right) \underline{L} \right]_{-1}^{1} = \left[\left(\frac{g}{2}(h_h)^2 - \frac{g}{2}(h_h)^2 \right) \underline{L} \right]_{-1}^{1} = 0 \,.
$$

Hence, $\frac{\Delta x}{2}\frac{d\underline{u}_2}{dt} = 0$, proving that the lake at rest situation is preserved.

6 CONCLUSIONS

While the higher degree of exactness of Gauss quadrature may or may not yield a more accurate numerical solution depending on the specific test case, a Fourier analyis more directly pinpoints the source of the deviation of the semi-discrete DG solution from the exact solution of a linear PDE. Higher accuracy of Gauss nodes then manifests itself in higher accuracy of the physically relevant eigenvalue. Secondly, in certain situations, higher accuracy alone is not satisfactory in itself but has to be combinable with the preservation of relevant physically properties. Here, we have shown that the same approach used to achieve kinetic energy preservation for the Euler equations in [1] may be used to obtain entropy preservation for the shallow water equations.

REFERENCES

[1] Ortleb, S. A kinetic energy preserving DG scheme based on Gauss-Legendre points. *J. Sci. Comput.* (2017) **71**:1135–1168.

[2] Del Rey Fernández, D. C., Boom, P. D. and Zingg, D. W. A generalized framework for nodal first derivative summation-by-parts operators. *J. Comput. Phys.* (2014) **266**:214–239.

[3] Kopriva, D. A. and Gassner, G. J. On the quadrature and weak form choices in collocation type discontinuous Galerkin spectral element methods. *J. Sci. Comput.* (2010) **44**:136–155.

[4] Gassner, G. J. and Kopriva, D. A. A comparison of the dispersion and dissipation errors of Gauss and Gauss-Lobatto discontinuous Galerkin spectral element methods. *SIAM J. Sci. Comput.* (2011) **33**:2560–2579.

[5] Bassi, F., Franchina, N., Ghidoni, A. and Rebay, S. A numerical investigation of a spectral-type nodal collocation discontinuous Galerkin approximation of the Euler and Navier-Stokes equations. *Int. J. Numer. Methods Fluids* (2013) **71**:1322–1339.

[6] Gassner, G. J. A kinetic energy preserving nodal discontinuous Galerkin spectral element method. *Int. J. Numer. Meth. Fluids* (2014) **76**:28–50.

[7] Bassi, F., and Rebay, S. Numerical evaluation of two discontinuous Galerkin methods for the compressible Navier-Stokes equations. *Int. J. Numer. Meth. Fluids* (2002) **40**:197–207.

[8] Zhang, M, Shu, C. W. An analysis of three different formulations of the discontinuous Galerkin method for diffusion equations. *Math. Models Meth. Appl. Sci.* (2003) **13**:395–413.

[9] Guo, W., Zhong, X. and Qiu, J. M. Superconvergence of discontinuous Galerkin and local discontinuous Galerkin methods: Eigen-structure analysis based on Fourier approach. *J. Comput. Phys.* (2013) **235**:458–485.

[10] Gassner, G. J., Winters A. R. and Kopriva, D. A. A well-balanced and entropy conservative discontinuous Galerkin spectral element method for the shallow water equations. *Appl. Math. Comput.* (2016) **272**:291–308.

[11] Ranocha, H. Shallow water equations: split-form, entropy stable, well-balanced, and positivity preserving numerical methods. *Int. J. Geomath.* (2017) **8**:85–133.